

jScan: Non-Invasive Technique for Bilirubin Quantification and Jaundice Detection

Kondury Rishabh, Pratyush Parashar, Debanjan Das, *Member, IEEE*, Venkanna U, *Member, IEEE*,

Abstract—Jaundice occurs due to excess deposition of bilirubin in the blood causing the yellow colouring of eyes, skin. The proposed paper presents jScan which is a novel Non-Invasive Autonomous Bilirubin Estimation technique to address the shortcomings of hyperbilirubinemia and jaundice prediction. The model captures the eye image and autonomously extracts the sclera as the region of interest using the smartphone camera. The Adaptive KMeans algorithm is used to find the dominant colour by analyzing color spectroscopy of the extracted portions and predicts the bilirubin level in the blood. A value greater than 3 mg/dl is classified as hyperbilirubinemic. The model predicts the bilirubin level to an accuracy of 88% and sensitivity of 0.93. Furthermore, a novel brightness adjustment algorithm is developed, allowing robustness to a wide illumination range and the type of device used. The model thereby establishes itself as an authentic and acceptable replacement for invasive and clinically-based bilirubin tests.

Keywords—Jaundice, Autonomous, Bilirubin, Image analysis, Non-invasive, Region of Interest, Machine learning.

I. INTRODUCTION

Jaundice is the yellowish pigmentation of the skin and whites of the eyes due to high bilirubin levels. Jaundice in adults is typically a sign indicating the presence of underlying diseases involving abnormal heme metabolism, liver dysfunction, or biliary-tract obstruction. The most commonly associated symptoms of jaundice are itchiness, yellowish colouration, and dark urine. The values of bilirubin in blood are normally below 1 mg/dl, which increases to over 3 mg/dl during jaundice. It causes an estimated 114k deaths and 178k cases of disability per year [1]. Due to jaundice being a major public health issue, its early detection is of critical importance.

The long-established regions predominantly used by physicians to infer if a patient has jaundice, during a physical examination are the sclera region, fingernail beds, face, palm region, and the volar surface. Out of all these regions, determination by the scleral region remain robust to the patient's race [2]. The overlaying conjunctiva region accumulates more bilirubin than the sclera [3] but in our case, the sclera and conjunctiva in combination are addressed as sclera. Eye conjunctiva has a

- Kondury Rishabh is with the Data Science and Artificial Intelligence Department, IIIT–Naya Raipur, Chhattisgarh 493661, India (e-mail: rishabh20102@iitnr.edu.in).

- Pratyush Parashar is with the Data Science and Artificial Intelligence Department, IIIT–Naya Raipur, Chhattisgarh 493661, India (e-mail: pratyush20102@iitnr.edu.in).

- Debanjan Das is with the Electronics and Communication Engineering Department, IIIT–Naya Raipur, Chhattisgarh 493661, India (e-mail: debanjan@iitnr.edu.in).

- Venkanna U is with the Computer Science and Engineering Department, IIIT–Naya Raipur, Chhattisgarh 493661, India (e-mail: venkanau@iitnr.edu.in).

particularly high affinity for bilirubin deposition due to high elastin content. Even slight increase in bilirubin value can be detected early by observing the yellowing of sclerae. The above mentioned reasons makes it optimal to choose sclera as the region of interest.

Blood bilirubin tests can be broadly categorized as invasive and non-invasive. The clinical method to estimate bilirubin levels by drawing blood is called Total Serum Bilirubin (TSB) test which is painful, time-consuming, potentially hazardous, requires trained professionals, and is both inaccessible and unaffordable, especially in rural and remote areas of the low and middle-income countries (LMC) where jaundice cases are more frequent. To overcome these shortcomings, in underdeveloped regions of the world, non-invasive techniques have operational advantages. Some non-invasive techniques like were developed, where the bilirubin value could be determined with similar accuracy and easily accessible as inexpensive medical devices. These devices made prompt mass screening and jaundice prediction in resource limited areas possible. There are, however, a few drawbacks in the non-invasive detection techniques. Some solutions like [4] [5] focus mostly on Neonatal jaundice and not on adult cases. Techniques like R-jaunlab [6] cannot be implemented on smartphones due to hardware limitations. The non-autonomous method in some solutions requires the user to select the best instances from the captured image, [7] require an expensive setup for bilirubin quantification.

In the proposed methodology, we have carefully aimed to remove all the shortcomings and contribute to the field of non-invasive jaundice detection, by making autonomously selecting the region of interest. We have developed a cross platform smartphone-based solution in the form of jScan. The integrated smartphone camera acts as sensors to capture an eye image and, the captured image's spectroscopy, is utilised to estimate the blood bilirubin level. This estimated bilirubin value is used to classify patients and predict jaundice. The collected dataset is appropriately balanced with a wide range of bilirubin values and age groups.

A. Contributions

The contributions of this paper are as follows:

- The proposed algorithm consists of a 3-step process for sclera segmentation
- To the best of our knowledge, this paper is the first work that involves a smartphone that implements full autonomous working and does not involve any manual intervention.

- The proposed algorithm can detect jaundice by measuring the bilirubin value of the eye by estimating the yellowness index of the sclera region of the eye. The method is tested on dataset in varying conditions and found to be reliable despite being resource-constrained.
- The measured Total Serum Bilirubin value has an accuracy of 88% and an error of ± 0.29 g dL⁻¹, compared to clinically measured value.
- The model performs well under normal lighting conditions and it does not require any additional equipment for its working.

The paper has the following structure – Section II covers the related prior works followed by the novelty of the paper. Section III describes the jScan architecture followed by the proposed methodology in Section IV. Section V illustrates the experimental study and Section VI discusses the results. Finally, section VII draws a compact conclusion and mentions the areas of future research.

II. RELATED WORKS

A. Related Prior Research Works

Bilirubin Quantification is classified in two categories invasive and non-invasive. According to [8], invasive procedure is done by deliberate access to the body via an inclusion. Invasive bilirubin tests like the gold standard method of Total Serum Bilirubin (TSB) are painful, high-cost and require trained medical professionals. The shortcomings of invasive tests can be overcome by using non-invasive methods. Many attempts have been made in developing invasive methods for jaundice prediction in the past. The use of Transcutaneous Bilirubinometer as mentioned in [9], [10] involves the use of phototherapy and avoids the usage of blood sampling. The above mentioned techniques require extra hardware for the measurement and it's unavailability, cost makes it unfit for common use. Further, Billicheck [10] was proposed, which uses multiwavelength spectral analysis for estimation of Transcutaneous bilirubin based on the skin colour. Choosing the sclera as the ROI increased the accuracy of the model due to the reasons mentioned in Introduction.

- Healthy sclera is white, independent of the ethnicity of the subject
- Sclera is less influenced by pigments such as melanin unlike skin
- Quantification of yellowness readily provides an estimation of bilirubin level

B. Novelty of the proposed technique

In this paper, we propose jScan, a non-invasive, self-sufficient, accurate, and smartphone implemented model. The smartphone and its camera function as sensors to capture and evaluate the captured image spectroscopy. jScan automatically extracts the sclera region of the eye using the proposed novel sclera-segmentation method, followed by the extraction of RGB code for the most dominant colour and predict the bilirubin value based on the spectroscopy information from the extracted regions. Finally, based on the calculated bilirubin

value, a prediction for jaundice is made. The accuracy of our model surpasses the accuracy of most of non-invasive jaundice detection techniques. The model is very lightweight, computationally fast and is developed using image processing techniques so that it can be easily incorporated in smartphones.

III. JSCAN: A SYSTEM LEVEL OVERVIEW OF THE PROPOSED TECHNIQUE

This section describes the proposed three-step technique for jaundice prediction, as shown in Fig.1. There are three main phases involved: Phase 1: Extracting the Region of Interest (ROI), Phase 2: Dominant colour extraction and Jaundice prediction, and Phase 3: jScan cross-platform mobile application. In Phase 2, a novel and efficient algorithm called NIABE (Non-Invasive Autonomous Bilirubin Estimation) is proposed. Following subsections explain each phase in detail of the proposed technique.

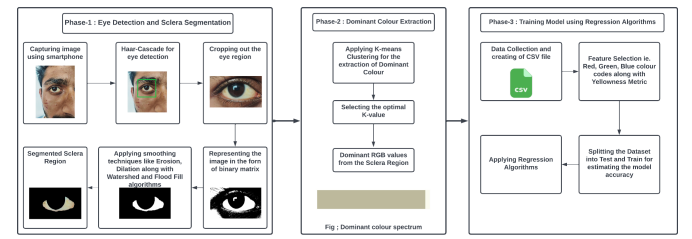


Fig. 1: Proposed Novel Smart Jaundice-Care Architecture

A. Phase 1: Extracting the Region of Interest

To obtain the ROI, we implement the GET_ROI algorithm. It takes the captured eye image of the patient as input and results the required sclera region of the eye as the region of interest. Algorithm 1 outlines the functioning of GET_ROI algorithm. The GET_ROI algorithm performs an ordered set of functions as shown in Fig. 3, each are explained as follows.

1) *Eye Detection:* The GET_ROI algorithm starts with the detection and extraction of the eye region from the captured image. For this, we use the Haar Cascade eye detector [?] (line 2, Algorithm 1). The Haar Cascade is a technique in which a cascade function trained using several positive and negative images, is used to identify the specific object of interest from other images. To train the algorithm several images with and without eyes are required. For each such image, features (F) are calculated as represented by equation (1),

$$F = \sum_{i \in BR} P_i - \sum_{j \in WR} P_j, \quad (1)$$

where, BR, WR are the black and white convolutional kernels and P_i , P_j the values of pixel i and j , respectively. Further,

TABLE I: Comparison of pre-existing techniques for Bilirubin estimation

Existing Technologies	Non-Invasive	Smartphone-based	No Additional equipment	Cost-Effective (< \$10)	Adults	Accurate (LOA < 3 g dL ⁻¹)	Autonomous
R-JaunLab [2]	✓	✗	✗	✗	✗	✗	Fully
Neonatal Jaundice via Ambient subtraction [3]	✓	✗	✗	✓	✗	✗	Semi
Total serum bilirubin test	✗	✗	✗	✗	✓	✓	Manual
Bilicheck [11]	✗	✗	✗	✗	✗	✓	Manual
Bilicam [12]	✓	✗	✗	✓	✗	✓	Fully
BiliScreen [4]	✓	✓	✗	✗	✓	✓	Semi
Jaundice Eye Colour Index (JECI) [5]	✓	✓	✓	✓	✓	✓	Fully
Neonatal Jaundice Screening [8]	✓	✓	✗	✗	✓	✓	Semi
Euclidian Distance DIP [9]	✓	✓	✗	✗	✓	✓	Semi
Smartphone Assesment of Jaundice [7]	✓	✓	✗	✗	✓	✓	Semi
jScan (our proposed method)	✓	✓	✓	✓	✓	✓	Fully

Algorithm 1 : GET_ROI

Input: img_orig
Output: ROI

```

1: ROI = ∅ {Initialize matrix as Null}
2: eyes = Haar Cascade Technique for eye detection
3: if eyes detected then
4:   ROI_reduced = cropped_eye(eyes)
5:   bin_eyes = convert_binary(ROI_reduced)
6:   sclera = morphological_operations(bin_eyes)
7:   for each row,column in sclera do
8:     if sclera[row,column] > 250 then
9:       sclera[row,column] = 255
10:    end if
11:   end for
12:   final_ROI = subtract sclera from img_orig
13: end if

```

to improve the time complexity, double integral on the input image is performed as given by equation (2),

$$I.g = \left(\int \int I \right).g'', \quad (2)$$

where I is the image, g is the rectangular kernel, and g'' is the double derivative of g first along the row and then column. Features are applied to all the training images and the best threshold is calculated based on the correct detection of an eye region. The process starts by assigning equal weights, which are either decreased or kept the same depending on the classification accuracy, after each iteration. The number of iterations and the desired error rate is hardcoded and the algorithm stops after it achieves either of them. The features with minimum error rate are stored to detect eye(s) from an image.

Every feature is assembled into different stages of classifiers. For an input image, a window region is selected and the first stage of classifiers is applied, comprising very few features. If it fails, the remaining stages are not applied. The window region that succeeds in all stages is classified as an eye region. The extracted eye region is passed on to the next step where the eye image is converted into grayscale image followed by resizing the dimensions of the image.

2) *Adaptive Gaussian Thresholding:* In this phase, the cropped out eye image is converted to binary image so that image processing operations can be performed on the image. The image is then assigned a threshold value, which decides whether the pixel would be 0 or 255. If the pixel value is greater than threshold, it is converted to 255(black) otherwise, it is converted to 0(white). The threshold value is selected by the use of adaptive Gaussian thresholding technique which does not use a global threshold value to take in consideration the varying lighting conditions. The threshold value for a pixel is determined by the small region around it by taking . The various threshold values are then applied on the image giving improved results for varying illumination conditions. The threshold value for a pixel is the weighted Gaussian sum of the neighbourhood values. Every pixel in the binary image, P_i is assigned a value given by equation (3),

$$P_i = 0 \quad \text{if } S(i, j) > T(i, j) \\ = 255 \quad \text{otherwise} \quad (3)$$

where, $T(i, j)$ is a threshold calculated individually for i th and j th pixel, $S(i, j)$ is the initial pixel value.

3) *Morphological Operations:* The next step is to perform morphological operations on the image for sclera segmentation. Various methods of image segmentation like erosion, dilation, watershed and flood-fill algorithm are being applied on the segmented sclera region. The techniques give the required ROI for further analysis. Figure 2 shows the implementation of the above mentioned technique.

4) *Masking and Image Subtraction:* After the sclera region is segmented out from the eye image, the image is then compared with the original image and an image mask is created using it. For each pixel, whenever a non-black colour is encountered, the region is assumed to be the sclera part and by taking all such pixels, sclera region is formed. The masked region has been coloured black, so the only coloured region to be subtracted the required ROI. Image subtraction can be stated as the pixel subtraction over all pixels between two images. The pixel subtraction operation inputs two images and outputs a third image whose pixel values are obtained by subtracting the second image from the first image. For example, if I_1, I_2 be the two images, I_3 the image formed from subtracting the two images and P_i, P_j, P_k denotes the

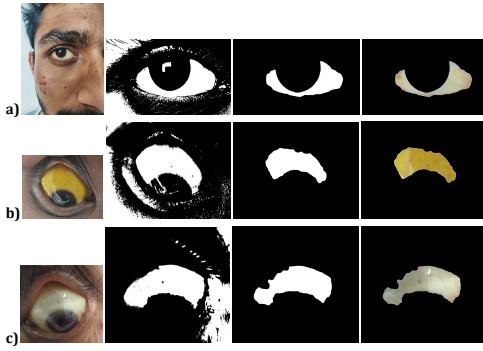


Fig. 2: Our novel and modified morphological and binarized gradient technique for the computation of the binary mask outperforms the simple gradient method. (a),(b),(c) are the morphological gradients and binary masks of three participants. **i** represent the regions upon which gradient techniques and masking have to be performed. **ii** and **iii** represent the morphological gradients and binary masks of three participants, respectively. **iv** represents the segmented sclera regions wherein the dominant color has to be calculated.

pixel value at point i, j, k respectively, then, mathematically we can write,

$$\begin{aligned} P_{i \in I_3} &= [P_{j \in I_1} - P_{k \in I_2}] \leftrightarrow P_{j \in I_1} - P_{k \in I_2} \geq 0 \\ &= 0 \quad \leftrightarrow P_{j \in I_1} - P_{k \in I_2} < 0. \end{aligned} \quad (4)$$

B. Phase 2: Yellowness Measure

The extracted ROI is now used to find the extent of yellowness in the sclera region to predict the bilirubin value. The RGB code for the extracted sclera is found by using KMeans clustering algorithm.

1) *KMeans Clustering Algorithm*: It is an unsupervised clustering technique, the data set of N points is divided into K clusters where each cluster has a greater similarity in an aspect than the other clusters. Here, the images' are clustered so, the similarity refers to the RGB code of the pixels. The mathematical intuition behind the KMeans clustering is forming clusters having minimum relative distance with other points from the center of the cluster, termed as "Cluster Center". For the image with resolution $N \times M$, there are NM data points, where each of the data-points consists of three components: red(R), green(B) and blue(B). Then the points are divided into K different clusters.

The value of K ie. the number of clusters differs for every image and has to be selected manually but, by using the Adaptive KMeans Clustering, the value of K can be automatically selected. The algorithm initializes a list called "Clusters" of size K , the i th index of the list denotes the center of the cluster. This is followed by initializing a list of $K \times N$ called "pt_list", where the i th index of pt_list is a set of similar cluster points having Clusters[i] as the cluster center (line 2, Algorithm 2). The first K points of the pre-processed dataset are appended to the Clusters list (line 3, Algorithm 2). Let cluster_num denote cluster number and N be the dataset size. For each point from the remaining $N-K$ data

points, the initial distance is set as infinity, cluster_num is set as -1. Let Cluster_center be the notation for each cluster center in Clusters. If x and y denotes the point and Cluster_center, the Euclidean distance E_d between them is given by Equation (5) (line 8, Algorithm 2),

$$E_d(x, y) = \sqrt{\sum_{p=1}^n (x_p - y_p)^2} \quad (5)$$

The value of the minimum Euclidian distance is replaced on each iteration. When program control returns outside the loop, the point under consideration gets appended to the index cluster_num in Pt_List (line 14, Algorithm 2). Then the new cluster centers are computed for the new set of points by iterating through each pt_idx in Pt_List and updating Clusters[pt_idx] as the mean of all points in Pt_List[pt_idx] (lines 15-17, Algorithm 2). The final calculated cluster center values are returned and selected as the dominant colour for the given ROI.

2) *Adaptive KMeans*: The traditional KMeans clustering requires manual selection of K value. Semi-manual methods like Elbow method and Silhouette methods are not useful in this case. Therefore, here we used Adaptive KMeans technique which takes into consideration four different clustering evaluation metrics. The initial value of K is set as 2 (minimum number of clusters required) and the four quality measurement indexes are initialized to null values. The value of K on each iteration is increased with the four quality measurement calculated for the current K value. When three or more indexes indicate unsatisfactory clustering marked by lower value compared to its previous one, the algorithm stops, and the previous K value gets returned as the optimal K value.

3) *Dominant Colour*: The dominant colour is estimated based on the clusters found by the method proposed in iNAP. The data is converted to RGB colorspace and stored as a list. The clusters formed from AdaptKMeans is used to plot RGB histogram. The colour with the maximum number of assignments is termed as dominant colour (due to highest frequency).

TABLE II: Bilirubin Levels based on Severity of Jaundice

Bilirubin Level (in mg dL ⁻¹)	Severity of Jaundice
3-8 mg dL ⁻¹	Mild
8-12 mg dL ⁻¹	Moderate
more than 12 mg dL ⁻¹	Severe

4) *Yellowness Index*: The yellowness index from the most dominant colour's RGB code is estimated by using HSL System Based Colour Clustering Algorithm [13]. proposes a construction of a new distance in the HSL color space by a combination of the distances of HSL scalar components and by using the fuzzy c-means framework to derive a fuzzy color clustering method. The technique converts the RGB colour into HSL colour space where H = hue, S = saturation, L = luminosity. The calculation for Hue and Saturation can be done using the Equation (6) and (7)

Algorithm 2 : Adaptive_KMeans**Input:** ROI**Output:** Optimal K value

- 1: **Clusters** = \emptyset {Initialize K size list for storing cluster centers}
- 2: **Pt_list** = KxN list
- 3: **Adding initial K data points as cluster centers**
- 4: **for** every Point in the Dataset **do**
- 5: **Distance** = INF
- 6: **Cluster_num** = initialized as -1
- 7: **for** every Point in the Dataset **do**
- 8: **Euclidian_distance** = Euclidian Distance between Point and Cluster
- 9: **if** Distance > **Euclidian_distance** **then**
- 10: **Cluster_num** = Update value to **Cluster_Center**
- 11: **Distance** = Update value to **Euclidian_Distance**
- 12: **end if**
- 13: **end for**
- 14: **Adding Point to Pt_list[Cluster_num]**
- 15: **for** every Point_idx in Pt_list **do**
- 16: **Clusters[Point_idx]** = Get the mean of all points in Pt_list[Point_idx]
- 17: **end for**
- 18: **end for**

$$H = \arctan\left(\frac{B - G}{\sqrt{2}}, \frac{2R - B - G}{\sqrt{6}}\right) \quad (6)$$

$$L = \frac{R + G + B}{3} \quad (7)$$

where, $H \in [-\pi, \pi]$

5) *Calculating the Bilirubin Value:* The Bi_Calculator algorithm is proposed and represented as Algorithm. The bilirubin values from the dataset is mapped with the yellowness index of the train split. Linear regression algorithm is applied using yellowness index as the input variable and bilirubin value as the output variable. The parameters are tuned manually according to the results of the prediction made to ensure optimum accuracy. The formula upon tuning the variables is represented in Equation (8).

$$\text{Bilirubin} = 0.46R - 0.32G - 0.01B - 37.22Y + 9.91 \quad (8)$$

Algorithm 3 : Bi_Calculator**Input:** ROIs**Output:** Bi

- 1: **r_int** = \emptyset , **g_int** = \emptyset , **b_int** = \emptyset {Initialize as Null}
- 2: **r** = 0, **g** = 0, **b** = 0 {Initialize as 0}
- 3: **for** each image in s_ROIs **do**
- 4: **Y** = Calculate **Yellowness_index**
- 5: **end for**
- 6: **Bi** = Calculate **Bi** using equation

6) *NIABE Algorithm:* The previously mentioned algorithms are merged into a single algorithm called NIABE (Non-Invasive Autonomous Bilirubin Estimation). The algorithm performs the task of extracting the region of interest: GET_ROI, finding the extent of yellowness Yellowness_Index and Bilirubin calculation: Bi_Calculator. The models are explained in detail in the phase diagram, in Fig 3. From the yellowness index, the Bilirubin value is calculated and the patient is classified as Hyperbilirubinemic or healthy. Algorithm illustrates the working of the NIABE algorithm.

Algorithm 4 : NIABE**Input:** img_orig**Output:** Jaundice or Healthy

- 1: **ROI** GET_ROI(img_orig)
- 2: **s_ROIs** = S_ROI(ROI)
- 3: **Bi** = Bilirubin_Calculator(s_ROIs)
- 4: **if** Bi > 3 mg/dl **then**
- 5: **Hyperbilirubinemic (Jaundice)**
- 6: **else**
- 7: **Healthy**
- 8: **end if**

Line 1 (Algorithm 1) passes the captured eye image to the GET_ROI function, to obtain the required ROI. Line 2 (Algorithm 1) passes the obtained ROI to the S_ROI function, to obtain the best segmented regions of the sclera. In line 3 (Algorithm 1) the set of best segments are passed to the Bi_Calculator function, to get the Bilirubin value of the patient. Once the bilirubin level is obtained, a patient is termed as Hyperbilirubinemic if the value is below 3 mg dL⁻¹ and healthy otherwise. Finally, the model is saved and then converted from .py (python) file to .apk (smartphone application) file.

TABLE III: Time Complexity of the Proposed Methodology

Phases of Proposed Methodology	Time Complexity
Eye Detection	0.2 s
Cropping of Eyebrows	0.16 s
Sclera Segmentation	1.24 s
Sclera Validation	1.08 s
Dominant Color Extraction	3.26 s
Color Spectrum Computation	1.12 s
Bilirubin Estimation	1.48 s

C. Phase 3: jScan App

The proposed model is implemented in a mobile application as the jScan app. A patient can measure his/her blood bilirubin value by downloading the app on the smartphone and capturing an eye image. The captured eye image is processed by the by the model hosted on cloud to first display the extracted sclera region as the region of interest, and then after analyzing the RGB values of that region, an estimation of bilirubin value is made which is later used to predict jaundice.

IV. EXPERIMENTAL STUDY

This section describes the dataset used for testing our model and the computational platforms used for building it.

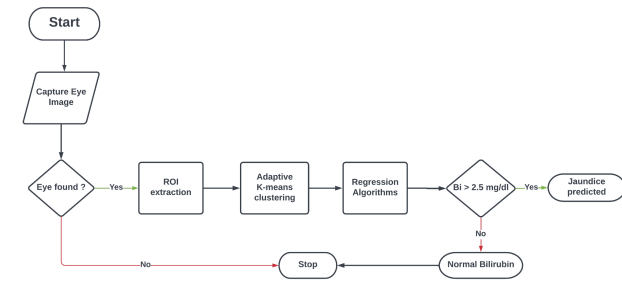


Fig. 3: Conceptual Flowchart of NIABE Algorithm



Fig. 4: Images excluded due to Improper Capturing

A. Dataset Used

For the experiment, 82 participants were approached over six weeks. Out of them, 7 refused to participate. The remaining 68 participants gave their verbal assent, written consent, and additional parents' permission (for minors, age < 18). The study had been approved by the Institute Ethics Committee (AIIMS/RPR/IEC/2020/1007) dated 22/03/2022 and the procedures were performed in full accordance with ethical principles and guidelines of Indian Medical Association. Out of the 75 participants, photographs for 7 participants were excluded because of technical reasons, and the photograph of only one eye was considered for 7 (four right eyes and three left eyes) participants. The main technical reasons for exclusion of photographs of the participants are:

- Eye pupil not properly focused (Fig. 4a, Fig. 4b)
- Low brightness leading to the inefficient execution of sclera segmentation. (Fig. 4c)
- Eyebrow region missing, thereby leading to the failure of eye detection (Fig. 4d)

For the remaining 61 participants both right and left eye was considered. The statistical information about the complete recorded dataset is given in Table IV.

For each participant, a blood sample was collected for the clinical assessment of blood bilirubin level. To get an idea of the sensitivity of our model, we classified participants in either of 2 classes: "Non-Jaundiced" if Bilirubin $< 2.5 \text{ mg dL}^{-1}$ and "Jaundiced" if Bilirubin $\geq 2.5.5 \text{ g dL}^{-1}$. For all our tests, we have applied the adaptive-K means clustering algorithm which gives us the dominant color of the segmented sclera along with the complete spectrum of colours available in the sclera. The clinical assessment of the blood bilirubin level was performed at All India Institute of Medical Sciences (Raipur, India).

B. Computing Platforms

For developing the proposed algorithm, Python (Python 3.10.4, Python Software Foundation) and OpenCV 4.5.5 have been used. For the statistical analyses, we used Microsoft

Excel 2010 (Microsoft Corporation, WA, USA). The algorithm was assimilated into a smartphone-based application in the form of an app. Integrated Development Environment (IDE) of Android Studio (Google) was put into operation to develop an application using the Flutter language along with integration with ML Toolkit, thus making it cross-platform for use on Android and iOS operating systems, respectively. The time taken to capture the eye image and predict the blood bilirubin value varied on average between 8 seconds to 20 seconds.

V. IMPLEMENTATION OF jSCAN USING EDGE COMPUTING PLATFORMS

This section discusses the results achieved by jScan on real life images, followed by a comparative measure of the model with some of the existing bilirubin estimation techniques.

A. Results

1) Sclera Segmentation: Figure 5 illustrates some sclera regions segmented by our algorithm autonomously. To further assess the accuracy of our algorithm in correctly extracting the sclera region, we took the help of certified physicians specializing in the treatment of patients with blood disorders and asked them to inspect the extracted region. Out of the 61 extracted ROIs, 47 of them were such that a proper prediction on the patient's blood bilirubin level could be made manually, 8 extractions were moderate and 6 were unsatisfactory. Thus, ~90.8% of the time our algorithm extracts the proper sclera region as the ROI. This illustrates the ability of our model to be self-sufficient.

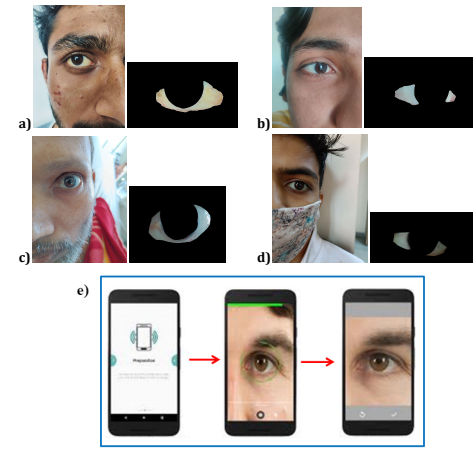


Fig. 5: a,b,c,d represents the segmented sclera regions as ROI. e represents the process of capturing an eye image by smartphone.

2) App predicts bilirubin level accurately for both eyes: We evaluated our model by measuring blood bilirubin levels for both the right and left eye. The pair of right and left eye images could be analyzed for 54 participants. The blood bilirubin level was measured for each eye separately, and then the average of them was considered to be the bilirubin level of the patient. The correlations with the actual blood bilirubin are very high when the average of both eyes are

TABLE IV: Statistical Information of Dataset used

Participant Information			Age (in years)				Gender		Blood Bilirubin (in mg dL ⁻¹)			
Total	Jaundiced	Non-Jaundiced	Range	Mean	Standard Deviation	95% Confidence Interval	Male	Female	Range	Mean	Standard Deviation	95% Confidence Interval
61	49	12	16 to 78	42	20	40 to 44	38	23	0.21 to 33.28	6.82	9.1	1.7 to 9.2

considered as illustrated by Fig. 6a. Figure 6b illustrates high correlations between measured bilirubin value using the left eye by NIABE and clinical laboratory tests, with the square of the correlation coefficient (R) equal to 0.93. Fig 7a illustrates high correlations between measured bilirubin value using the right eye and clinical laboratory tests, with $R^2 = 0.985$. This indicates that the predicted bilirubin values for each eye of individual patients, has high correlations with their clinically obtained blood bilirubin values from the CBC reports. The mean difference between the blood bilirubin level of the left and right eye is depicted in Fig. 7 b. The certainty that our model is reliable in terms of blood bilirubin level measurement, is further strengthened by the fact that the difference between the blood bilirubin levels measured for both eyes, for the same individual, vary within a reasonable limit of 0 to 5.8 g dL⁻¹ (mean difference = 2.14 g dL⁻¹).

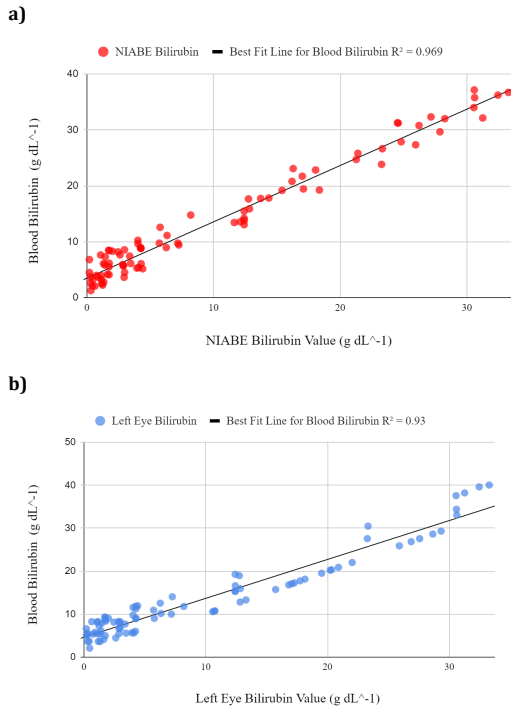


Fig. 6: a) High correlations between predicted bilirubin level and clinically measured bilirubin level. b),High correlations between measured left eye bilirubin values by NIABE and clinical lab tests.

3) Accurate Blood Bilirubin Measurement by jScan: The proposed model can function as an autonomous, non-invasive jaundice screening tool at regions where jaundice is rampant. It inputs only a single smartphone image of the eye and requires no manual intervention after that. Fig 6a illustrates

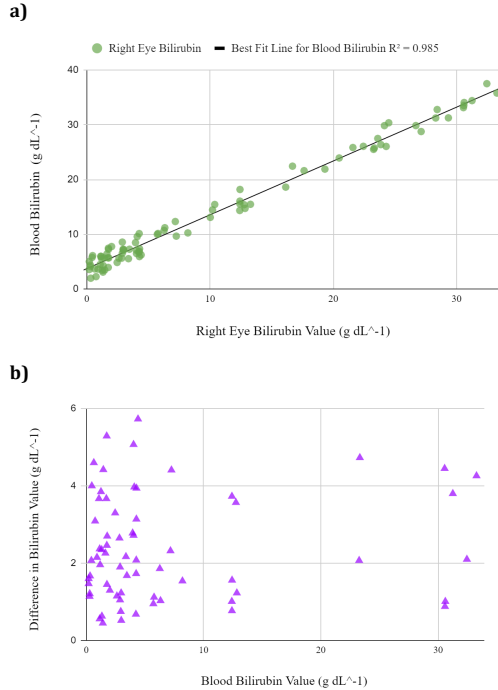


Fig. 7: a) High correlations between measured right eye bilirubin values by NIABE and clinical lab tests. b) Structured comparison between measured bilirubin level difference between left and right eye and the actual blood bilirubin level.

the model's strong correlation with the clinical laboratory tests. The solid line indicates the actual data fit between predicted bilirubin level and clinically measured bilirubin level. High correlations are observed between them with $R^2 = 0.969$. The Bland-Altman analysis in Fig. 9a demonstrates that the bilirubin measurement performed by NIABE has a minimal experimental bias of 2.14 g dL⁻¹ and narrow 95% limits of agreement (LOA) of [-0.82, 1.11 g dL⁻¹]. The solid red line indicates bias (2.14 g dL⁻¹) while dashed red lines represent 95% limits of agreement [-0.82, 1.11 g dL⁻¹]. In other words, bilirubin levels are predicted with an accuracy of ± 0.29 g dL⁻¹ and with a bias of 2.14 g dL⁻¹ of clinically measured bilirubin level, for 61 patients containing both individuals affected and unaffected by jaundice. All clinically accepted diagnostic tools for jaundice screening are required to have the 95% LOA within ± 2 g dL⁻¹ and our model satisfies the condition. The mean error (= 0.29 g dL⁻¹) is slightly higher than the model in [14]. However the error still lies within acceptable limits (< 1 g dL⁻¹) and is lower than the existing

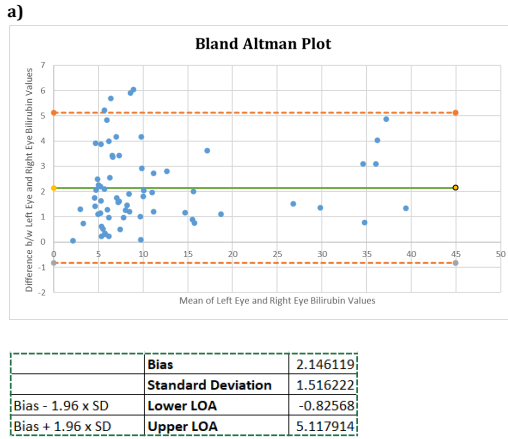


Fig. 8: a) Bland–Altman Plot on Bilirubin Measurement.

model. Testing the model on a larger dataset will result in an even smaller value of error. All these findings illustrate the accuracy of blood bilirubin measurement by jScan.

TABLE V: Confusion Matrix of the Classification based on Dataset

Predicted Condition	Actual Condition		$\frac{TP}{TP+FN}$	$\frac{FN}{TP+FN}$	Sensitivity
	Jaundice	No Jaundice			
Jaundice	44	2	0.8979	0.102	0.9362
No Jaundice	5	10			

Table V illustrates the prediction accuracy of our proposed algorithm. Using 11.5 g dL^{-1} as the demarcation value, the False Negative Rate (False Negative (FN)/[True Positive (TP) + False Negative (FN)]) and True Positive Rate (True Positive (TP)/[True Positive (TP) + False Negative (FN)]) for our model are obtained as 0.102 and 0.8979 respectively. Finally, the sensitivity of our model ($[1 - \text{False Negative Rate}]/\text{True Positive Rate}$) is measured to be equal to 0.9362, which demonstrates that the proposed model attained a very high jaundice screening performance.

4) *App functions well for any smartphone:* We captured images from two different mobile equipments, Oppo F15 having Android 11 as the operating system and iPhone 5 having iOS 10.3.4 as the operating system. As observed, the correlations between the bilirubin level measured by our model and the clinical test is very high for both the Android ($R^2 = 0.8293$) and iOS ($R^2 = 0.8732$) smartphones. Phases of jScan, namely bilirubin estimation and sclera segmentation have also been tested using cameras with qualities varying from 2 to 108 megapixels, as demonstrated in Fig.9. Results from these tests conclude that any smartphone can be used for capturing an eye image by focusing well. This strengthens the fact that our model will perform better in real-file scenarios as we aim to make the model smartphone implemented.

5) *Optimum Lighting Conditions:* Our model is robust to a wide range of illumination. To illustrate, we captured the eye image of one specific participant in 13 different lighting

TABLE VI: Result using Different Regression Algorithms

Regression Algorithm	MAE	MSE	RMSE
Decision Tree Regression	0.89	0.96	1.62
Random Forest Regression	0.67	0.78	1.18
Adaboost Regression	0.72	0.84	0.78
XGBoost Regression	0.53	0.94	0.52
RANSAC Regression	0.81	0.56	0.39
Multiple Linear Regression	0.38	0.44	0.26

conditions. The algorithm performed accurately for an illumination range of 900 to 2400 lux, and reasonably accurately for an illumination range of 700 to 3500 lux. Illumination in a normal household typically varies from 1200 to 1800 lux, and the algorithm predicts with the highest accuracy within this range.

We plotted the variation in accuracy of the model's prediction by running the Adaptive K Means Clustering Algorithm on pictures clicked within different ranges of illumination. Maximum accuracy is obtained when the pictures are clicked within the illumination range of 1200 to 2500 lux. We need a bit higher illumination range for the accuracy of the NIABE algorithm as we need distinct boundaries for the segmentation of the sclera which is taking place by making use of the principles of binary masking. However, due to the large number of pixels to be processed, the algorithm's computation time increases. Therefore for the optimum time complexity for the processing of the algorithm, an idea about the computation time is also required. We observed that the algorithm's computation is relatively faster when resized images are considered. Resizing the image should be done to an extent such that the processor can deal with the computation within optimum time. At the same time, we must not compromise the accuracy of the NIABE algorithm as it has medical applications wherein accuracy needs to be top notch. Hence, by integrating the information we have derived, we can get the optimum range for the resizing of images. To be even more precise, we would state that the extent to which we are resizing images in jScan gives us an accuracy of 88% and takes an average computation time of 8.54 seconds for an image of the resolution 1024 x 1024 with a size of 3.1 MB.

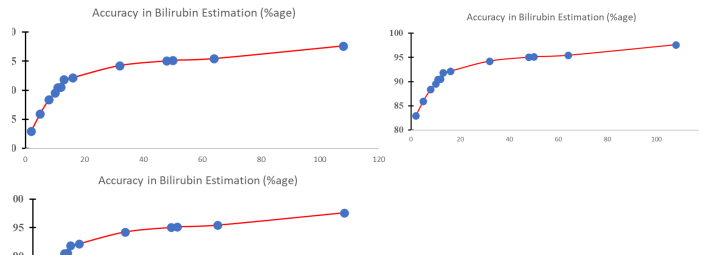


Fig. 9: a) Variation in Accuracy of Bilirubin Estimation with varying Camera Quality (measured in MP) b) Variation in Accuracy of Sclera Segmentation with varying Camera Quality (measured in MP)

B. Comparison With Existing Research

The proposed method achieved an accuracy of $\pm 0.29 \text{ g dL}^{-1}$ and a bias of 2.14 g dL^{-1} compared to gold standard

TABLE VII: Accuracy comparison with existing techniques

Method	Testing Size	95% LOA
R-JaunLab [15]	20	$\pm 3.7 \text{ g dL}^{-1}$
Neonatal Jaundice [14]	31	$\pm 3.6 \text{ g dL}^{-1}$
Non-Invasive Technique [16]	47	$\pm 3.5 \text{ g dL}^{-1}$
Smartphone Assessment of Jaundice [17]	19	$\pm 3.5 \text{ g dL}^{-1}$
BiliScreen [18]	27	$\pm 3.3 \text{ g dL}^{-1}$
Jaundice Eye Color Index (JECI) [19]	100	$\pm 2.7 \text{ g dL}^{-1}$
Neonatal Jaundice Screening [20]	144	$\pm 2.6 \text{ g dL}^{-1}$
Euclidean Distance DIP [21]	15	$\pm 2.5 \text{ g dL}^{-1}$
jScan	61	$\pm 1.93 \text{ g dL}^{-1}$

jaundice levels. In terms of accuracy, this is significantly higher than existing bilirubin tests such as the R-JaunLab: Automatic Multi-Class Recognition of Jaundice [15], smartphone screening for neonatal jaundice [14], and the non-invasive as well as more expensive bilirubin detection Technique for jaundice prediction using smartphones [16]. The model does not require any additional equipment to be attached to the smartphone, which improves cost-effectiveness compared to BiliScreen [18], Jaundice Eye Color Index (JECI) [19], and Methods for Determining Bilirubin Level in Neonatal Jaundice Screening and Monitoring [20]. Our model achieved a 95% limit of agreement $\pm 1.93 \text{ g dL}^{-1}$, which is significantly higher than existing techniques such as euclidean distance digital image processing for jaundice detect [21] and smartphone assessment of jaundice in liver patients [17] ($\text{LOA} > 2 \text{ g dL}^{-1}$). Finally, our algorithm is fully autonomous and does not involve any manual intervention while selecting the region of interest or best regions for extracting the RGB information. This is a major advantage over the existing non-autonomous techniques. The accuracy of each existing technique along with the size of the respective testing dataset is as illustrated in Table VII. Our model shows considerable improvement with respect to the accuracy.

VI. CONCLUSION AND FUTURE WORKS

Considering the omnipresence and ever-expanding rate of smartphone usage globally, the proposed model permits individuals at a high risk of jaundice to regularly monitor their health using their smartphones. The novel algorithm automatically extracts the sclera as a region of interest, measures the jaundice based on that image, and makes a prediction depending on the measured bilirubin value. jScan measures blood bilirubin levels to within $\pm 0.29 \text{ g dL}^{-1}$ of the actual blood bilirubin level, and screens jaundice with a sensitivity of 93.62%. The results achieved in our study portrays the reliability of the model and the prospect of using it as an jaundice screening tool over mass populations, especially in areas where there is a paucity of state-of-the-art laboratory facilities and professionals. Assessment on a larger dataset is likely to improve the model's accuracy further.

The concept of autonomous ROI extraction can be utilized to extract mucous membranes in parallel with the sclera, and then measure the blood bilirubin level using both the regions. For increased accuracy in the process of sclera segmentation, computationally expensive algorithms such as convolutional

neural networks and deep learning methods can be used. Improved sclera segmentation will lead to enhanced accuracy in bilirubin estimation. The prospect of implementing such computationally expensive algorithms using smartphones, in collaboration with image processing, can be explored.

REFERENCES

- [1] V. Bhutani, A. Zipursky, H. Blencowe, R. Khanna, M. Sgro, F. Ebbesen, J. Bell, R. Mori, T. Slusher, N. Fahmy, V. Paul, L. Du, A. Okolo, M. F. de Almeida, B. Olusanya, S. Cousens, and J. Lawn, "Neonatal hyperbilirubinemia and rhesus disease of the newborn: incidence and impairment estimates for 2010 at regional and global levels," *Pediatric research*, vol. 70 Suppl 1, pp. 86–100, 12 2013.
- [2] A. Bashkatov, E. Genina, V. Kochubey, and V. Tuchin, "Optical properties of human sclera in spectral range 370–2500 nm," *Optics and Spectroscopy*, vol. 109, pp. 197–204, 08 2010.
- [3] J. Kuiper, "Conjunctival icterus," *Annals of internal medicine*, vol. 134, pp. 345–6, 03 2001.
- [4] T. Leung, K. Kapur, A. Guilliam, J. Okell, B. Lim, L. Macdonald, and J. Meek, "Screening neonatal jaundice based on the sclera color of the eye using digital photography," *Biomedical Optics Express*, vol. 6, p. 4529, 11 2015.
- [5] A. Halder, M. Banerjee, S. Singh, A. Adhikari, P. K. Sarkar, A. M. Bhattacharya, P. Chakrabarti, D. Bhattacharyya, A. K. Mallick, and S. K. Pal, "A novel whole spectrum-based non-invasive screening device for neonatal hyperbilirubinemia," *IEEE Journal of Biomedical and Health Informatics*, vol. 23, no. 6, pp. 2347–2353, 2019.
- [6] Z. Wang, Y. Xiao, F. Weng, X. Li, D. Zhu, F. Lu, X. Liu, M. Hou, and Y. Meng, "R-jaunlab: Automatic multi-class recognition of jaundice on photos of subjects with region annotation networks," *Journal of Digital Imaging*, vol. 34, 02 2021.
- [7] M. M. M. Miah, R. Tazim, F. Johora, M. Imran, S. Surma, F. Islam, R. Shabab, C. Shahnaz, and A. Subhana, "Non-invasive bilirubin level quantification and jaundice detection by sclera image processing," 10 2019, pp. 1–7.
- [8] S. Cousins, N. Blencowe, and J. Blazebry, "What is an invasive procedure? a definition to inform study design, evidence synthesis and research tracking," *BMJ Open*, vol. 9, p. e028576, 07 2019.
- [9] J. Grabenhenrich, L. Grabenhenrich, C. Bührer, and M. Berns, "Tran-scutaneous bilirubin after phototherapy in term and preterm infants," *Pediatrics*, vol. 134, 10 2014.
- [10] D. Kumar, "Non-invasive bilirubin detection technique for jaundice prediction using smartphones," *International Journal of Computer Science and Information Security*, 08 2016.
- [11] F. Hemmati and N. Rad, "The value of bilicheck® as a screening tool for neonatal jaundice in the south of iran," *Iranian journal of medical sciences*, vol. 38, pp. 122–8, 06 2013.
- [12] L. Greef, M. Goel, M. Seo, E. Larson, J. Stout, J. Taylor, and S. Patel, "Bilicam: Using mobile phones to monitor newborn jaundice," *UbiComp 2014 - Proceedings of the 2014 ACM International Joint Conference on Pervasive and Ubiquitous Computing*, pp. 331–342, 09 2014.
- [13] V. Patrascu, "New framework of hsl system based color clustering algorithm," 09 2013.
- [14] F. Outlaw, M. Nixon-Hill, O. Odeyemi, L. Macdonald, J. Meek, and T. Leung, "Smartphone screening for neonatal jaundice via ambient-subtracted sclera chromaticity," *PLOS ONE*, vol. 15, p. e0216970, 03 2020.
- [15] Z. Wang, Y. Xiao, F. Weng, X. Li, D. Zhu, F. Lu, X. Liu, M. Hou, and Y. Meng, "R-jaunlab: Automatic multi-class recognition of jaundice on photos of subjects with region annotation networks," *Journal of Digital Imaging*, vol. 34, 02 2021.
- [16] N. Saini, D. Kumar, and P. Khera, "Non-invasive bilirubin detection technique for jaundice prediction using smartphones," *International Journal of Computer Science and Information Security*, vol. 14, pp. 1060–1065, 08 2016.
- [17] M. Nixon-Hill, F. Outlaw, L. Macdonald, R. Mookerjee, and T. Leung, "Minimising ambient illumination via ambient subtraction: smartphone assessment of jaundice in liver patients via sclera images," *Color and Imaging Conference*, vol. 2020, pp. 307–312, 11 2020.
- [18] A. Mariakakis, M. Banks, L. Phillipi, L. Yu, J. Taylor, and S. Patel, "Biliscreen: Smartphone-based scleral jaundice monitoring for liver and pancreatic disorders," *Proceedings of the ACM on Interactive, Mobile, Wearable and Ubiquitous Technologies*, vol. 1, pp. 1–26, 06 2017.

- [19] T. Leung, F. Outlaw, L. Macdonald, and J. Meek, "Jaundice eye color index (jeci): quantifying the yellowness of the sclera in jaundiced neonates with digital photography," *Biomedical Optics Express*, vol. 10, p. 1250, 03 2019.
- [20] F. Dzulkifli, M. Mashor, and K. Khalid, "Methods for determining bilirubin level in neonatal jaundice screening and monitoring: A literature review," vol. 10, pp. 1–10, 12 2018.
- [21] E. Rahayu, M. Widyawati, and S. Suryono, "Euclidean distance digital image processing for jaundice detect," *IOP Conference Series: Materials Science and Engineering*, vol. 1108, p. 012022, 03 2021.



Pratyush Parashar is an undergraduate of the Data Science and Artificial Intelligence Department at International Institute of Information Technology, Naya Raipur and will be graduating in 2024 with a B. Tech in Data Science and Artificial Intelligence. His current research interests include Computer Vision, Data Science, and Machine Learning.



Kondury Rishabh is an undergraduate of the Data Science and Artificial Intelligence Department at International Institute of Information Technology, Naya Raipur and will be graduating in 2024 with a B. Tech in Data Science and Artificial Intelligence. His current research interests include Algorithms Design, Computer Vision, Data Science, and Machine Learning.



Debanjan Das (M'10) received the B.Tech. degree in applied Electronics and Instrumentation engineering from the Heritage Institute of Technology, Kolkata, in 2009, the M.Tech. degree in Instrumentation from Indian Institute of Technology, Kharagpur, in 2011, and the Ph.D. degree in Electrical Engineering from Indian Institute of Technology, Kharagpur, in 2016. He is an Assistant Professor with Dr. SPM IIIT Naya Raipur. His current research interests include IoT-Smart Sensing, Signal Processing, Bioimpedance, Instrumentation.



Venkanna Udutoalapally (M'15) obtained his Ph.D. degree by the National Institute of Technology, Tiruchirappalli (NITT), in 2015. Since 2005, he has been in the teaching profession and currently he is an Assistant Professor in the Department of CSE, IIIT Naya Raipur (IIT- NR). He has eight years of teaching experience and seven years of research experience. His research interests include Internet of Things (IoT), Software Defined Networks, Network Security, Wireless Ad hoc, and Sensor network. He is a recipient of best paper award in IEEE-ANTS-2019 conference.